Supporting Information for

The effect of salt and particle concentration on the dynamic self-assembly of detonation nanodiamonds in water

Samir A. El-Demrdash [1], Reece Nixon-Luke[1], Lars Thomsen[2], Anton Tadich[2], Desmond W.M. Lau[3], Shery L. Y. Chang[4], Tamar Greaves[1], Gary Bryant[1], Philipp Reineck[5]

[1] *School of Science, RMIT University, Melbourne, Australia*
[2] *Australian Synchrotron, ANSTO, Clayton, Victoria, Australia*
[3] *RMIT Microscopy and Microanalysis Facility (RMMF), RMIT University, Melbourne, VIC 3001, Australia*
[4] *Electron Microscopy Unit, Mark Wainwright Analytical Centre and School of Materials Science and Engineering, University of New South Wales, Sydney, NSW 2052, Australia*
[5] *ARC Centre of Excellence for Nanoscale BioPhotonics, School of Science, RMIT University, Melbourne, Australia.*

Characterization of detonation nanodiamonds

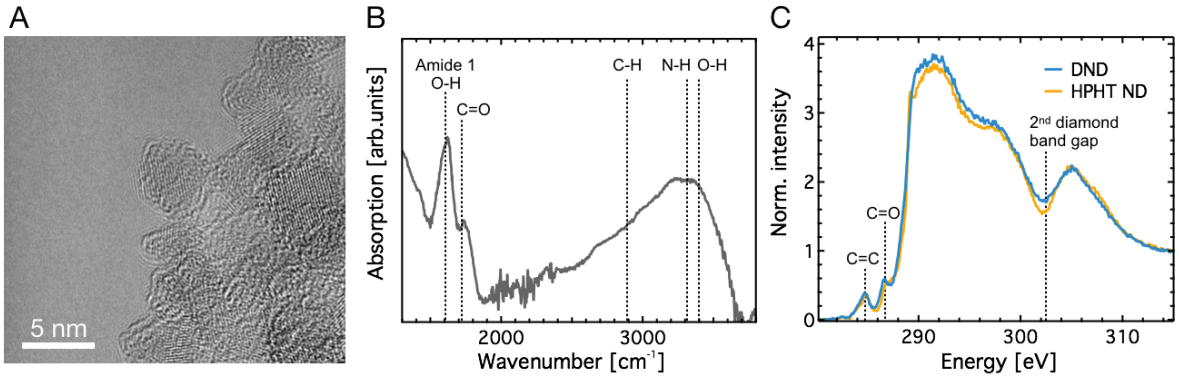

Figure S1: Physico-chemical characterization of detonation nanodiamonds. A: Transmission electron microscopy images of the DND particles. Primary particles of ~ 5 nm in diameter can be seen as part of a larger particle aggregate. B: Fourier transform infrared (FTIR) spectrum of the DND particles indicating the presence of several surface groups including carboxyl, hydroxyl and amine groups. C: Near-edge X-ray absorption fine structure (NEXAFS) spectra of the carbon K-edge of DND particles compared to high-pressure high-temperature (HPHT) nanodiamond particles. A pronounced second diamond band gap and relatively weak contribution from sp^2-hybridized carbon (C=C) show that most carbon is present in the form of sp^3 hybridised diamond. A significant peak at 287 eV indicates the presence of oxygen-containing surface groups.

Sample preparation

The diamond particles [4 mg/mL] were mixed with ion exchange resin for 24 h to remove the charged species, and the cleaned solution was transferred to a clean tube and diluted 1:1 with 0.02 mM NaCl, resulting in a stock solution consisting of 2 mg/mL DND particles in 0.01 mM NaCl. By diluting the stock solution in 0.01 mM NaCl we prepared a range of DND concentrations as shown in table S1. A similar procedure was applied to prepare samples at constant DND concentration with varying NaCl concentrations.

Table S1: DND concentration series

Sample No	Stock solution [µL]	0.01mM NaCL [µL]	DND conc. [mg/mL]
N1	3000	0	2
N2	1500	1500	1
N3	750	2250	0.5
N4	300	2700	0.25
N5	150	2850	0.1
N6	75	2925	0.05
N7	30	2970	0.025
N8	15	2985	0.01

DLS experiments

For DLS experiments, samples were transferred to cylindrical glass light scattering cuvettes and placed in the temperature controlled (294 K) ethanol bath in the DLS goniometer. For experiments involving sonication to disrupt DND aggregates, an ultrasonic probe sonicator (FS-600N ultrasonic homogenizer, Zhengzhou HengChen Electronic Co. Ltd., China) was operated at 100 W and 100% duty cycle.

Zeta potential measurements

Zeta potentials were measured with a Zetasizer ZS Nano (Malvern Instruments, UK). The instrument applies an alternating electric field across the sample, and the measured particle velocity is converted to the zeta-potential based on Henry's theory[1]. Using disposable folded capillary cells (DTS1070, Malvern Instruments, UK), measurements were performed at 294 K and the average and standard deviation from 3 measurements are reported.

SAXS experiments

Samples for SAXS were placed into 1.5 mm quartz glass capillaries (Hilgenberg, Germany) and sealed using beeswax. Measurements were carried out at room temperature, the acquisition time was 1 s for each measurement and each measurement repeated 10 times to ensure that the beam did not change the sample properties. Samples containing only the suspending solvent were also measured to determine the background scattering. The 2D SAXS patterns were converted to intensity vs scattering vector (q) and background corrected using the in-built software ScatterBrain*. Further analysis was carried out using SasView Version 5.0.3. [2]

* http://archive.synchrotron.org.au/aussyncbeamlines/saxswaxs/software-saxswaxs

Correlation function analysis

In this part we introduce different strategies for data analysis.[3] In short, monomodal size population and non-monomodal size population methods provide two different fitting approaches to extract reliable and robust results.

Exponential fitting: To approximate the observed behaviour of the correlation functions as 1 or 2 components, the correlation function is analysed using either a single exponential or biexponential model for the electric field autocorrelation function $g_1\ (q,\tau)$:

$$g_1(q,\tau) = e^{-\Gamma\tau} \qquad (1)$$

$$g_1\ (q,\tau)\ =\ a_0 + \ a_1 e^{\ -\Gamma_1\tau}\ +\ a_2\ e^{\ -\Gamma_2\tau} \qquad (2)$$

where τ is the delay time, $q = \frac{4\pi n}{\lambda} sin\left(\frac{\theta}{2}\right)$ is the magnitude of the scattering vector, n is the refractive index of the solvent, l is the laser wavelength, q is the scattering angle. The fit parameters are the decay constants Γ, Γ_1, Γ_2 are related to the diffusion coefficients by $\Gamma = q^2 D$. The relative amplitudes of the components are given by a_1, a_2. The particle diameters d can then be calculated using the Stokes-Einstein equation:

$$d = \frac{k_B T}{3\pi\eta D} \qquad (3)$$

Examples of the resulting fits are shown in Figure S2, demonstrating that the data cannot be fit using single exponential, but is well fit using the biexponential model.

Distribution fitting: For a polydisperse system, $g_1\ (q,\tau)$ will be an intensity-weighed integral over a distribution of decay rates $G(\Gamma)$ [4]:

$$g_1(q,\tau) = \int_0^\infty G(\Gamma) e^{-\Gamma\tau}\, d\Gamma \qquad (4)$$

Then using the Stokes-Einstein equation $G(\Gamma)$ can be converted to a distribution of particles sizes as shown in the main text. The analysis was carried out using the in-built ALV Correlator Software version 3 [5] using the CONTIN algorithm. [6, 7]

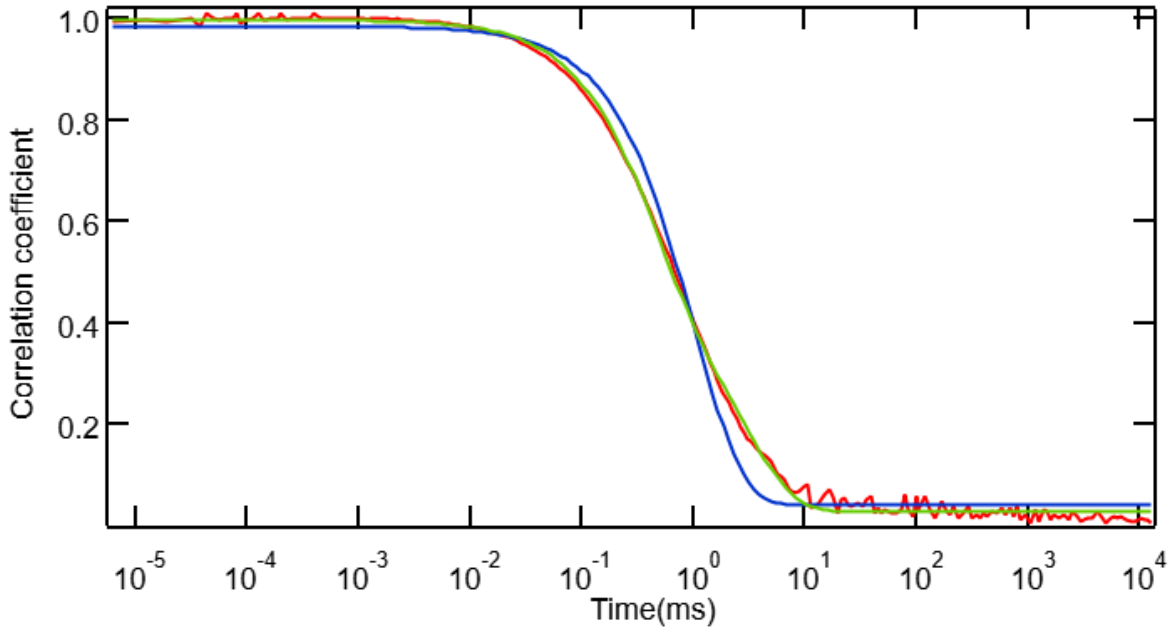

Figure S2: Representative correlation function (red trace) and fits using single exponential (blue trace) and biexponential (green trace). The single exponential fit is not a good representation of the data, but the biexponential provides a very good fit over the whole range.

Multi-angle DLS

In Figure S3 we report the results of multi angle DLS data measured over the angular range 12° - 140 ° at two DND concentrations of 2 mg/mL (A,B) and 0.025 mg/mL (C, D). At each angle the data can be fit by two representative decay times Γ_1 and Γ_2. Plotting the fitted Γ as a function of q^2 τ shows linear behaviour, and this q^2 scaling demonstrates that the biexponential decay is a good representation of the data over most of the angular range, highlighting the robustness of the analysis.[8] The lines show fits to the data over the range where linearity occurs. These correspond to diameter values of 266.5±18.2 nm and 29.6 ±0.9 nm for sample concentration 2 mg/mL and 302 ± 34 nm and 51.5±1.18 nm for sample concentration 0.025 mg/mL, which are consistent with the single angle analysis shown in the main text.

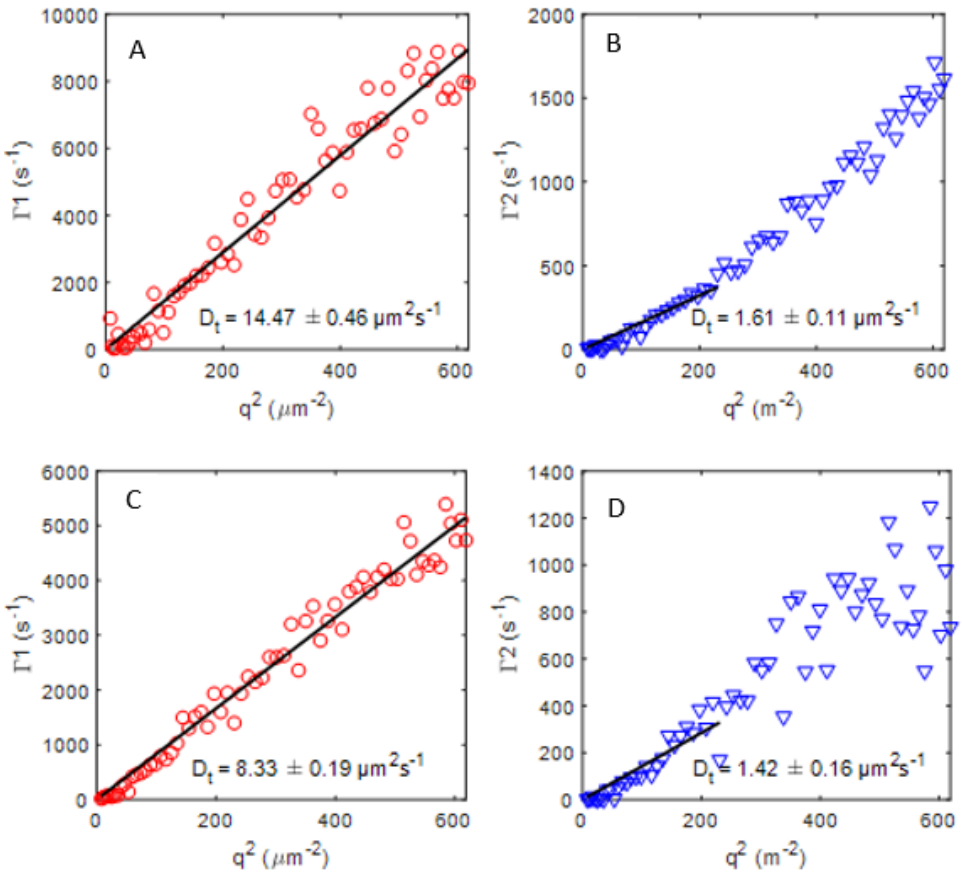

Figure S3. Multi-angle light scattering experiments. Relaxation rate of the correlation function versus the square of scattering vector (q^2) for DND concentrations of 2 mg/mL (A,B) and 0.025 mg/mL (C, D). Relaxation rates are for the small (red - A, C) and large (blue - B, D) aggregates respectively.

Table S2: NaCl and DND particle concentration of the samples shown in Figure S4 and Figure S7.

Sample ID	NaCL Conc. [mM]	DND conc. [mg/mL]
S1	9	0.1
S2	1	0.1
S3	0.5	0.1
S4	0.1	0.1
S5	0.05	0.1
S6	0.01	0.1
S7	0.005	0.1

Figure S4: Photographic images of the DND suspensions (0.1 mg mL^{-1}) with different ionic strengths, at higher salt concentrations (S1) the ND particles aggregated strongly and precipitated as shown.

SAXS data analysis

The SAXS data were analysed using the Guinier-Porod model[9] implemented in SasView. The Guinier-Porod model is an empirical model which can be used to determine the dimensionality of scattering objects and obtain information about their shapes. Three parameters are involved in the fitting process: the radius of gyration (R_g), the Porod exponent (d) and the dimension variable (s). In order to reduce the number of parameters, and given we know the approximate size of the primary DNDs, we fix R_g = 5 nm and allow the other parameters to vary.

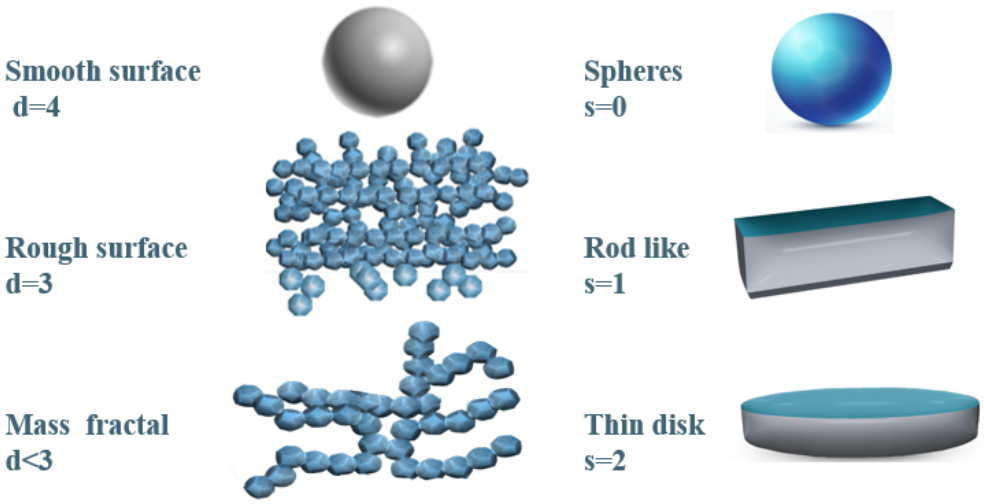

Figure S5: Schematic illustration of the shape and structure of simplified objects that correspond to selected Porod exponents (d) and dimension variables (S) based on the Guiner-Porod model[9].

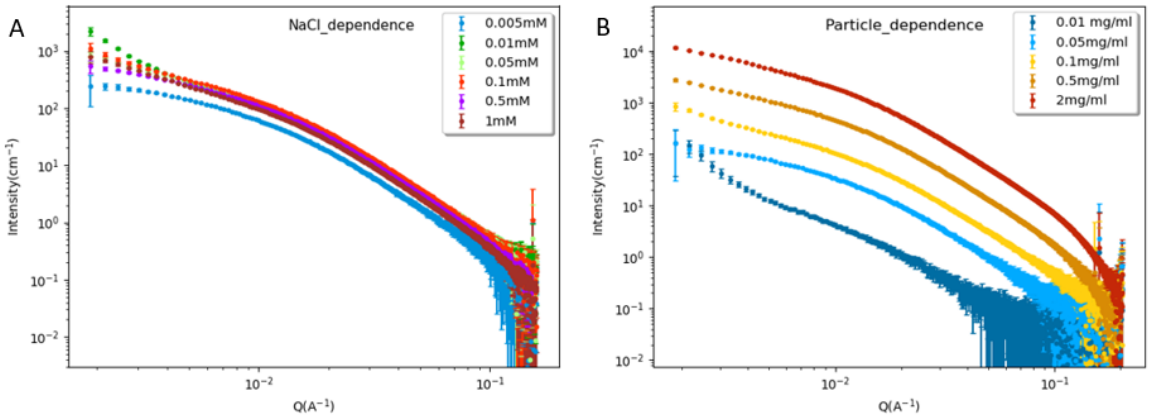

Figure S6: Primary experimental data for diamond nanoparticles A: DND SAXS profiles measured in solution with a salt concentration ranging from 0.05 mM to 1 mM and a fixed DND concentration 0.1 mg/mL B:DND SAXS profiles measured in solution with a concentration ranging from 0.01 mg/mL and 2 mg/mL at constant ionic strength(0.01mM NaCl).

The effect of salt concentration on the shape of the DND aggregates

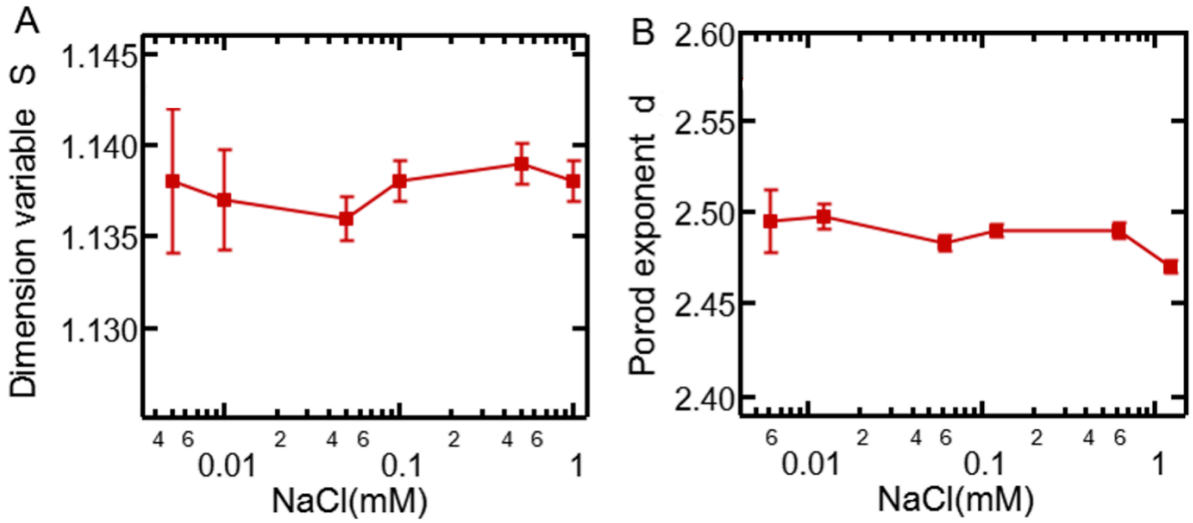

Figure S7: Aggregate shape parameters determined from SAXS data. Fits are constrained with a primary size of R_g = 5 nm. (A) shows the dimension variable S and (B) shows the Porod exponent d as a function of NaCl concentration. The data shows that neither the dimension variable S (A) nor the Porod exponent d (B) change with salt concentration.

The effect of pH change on the shape of the DND aggregates

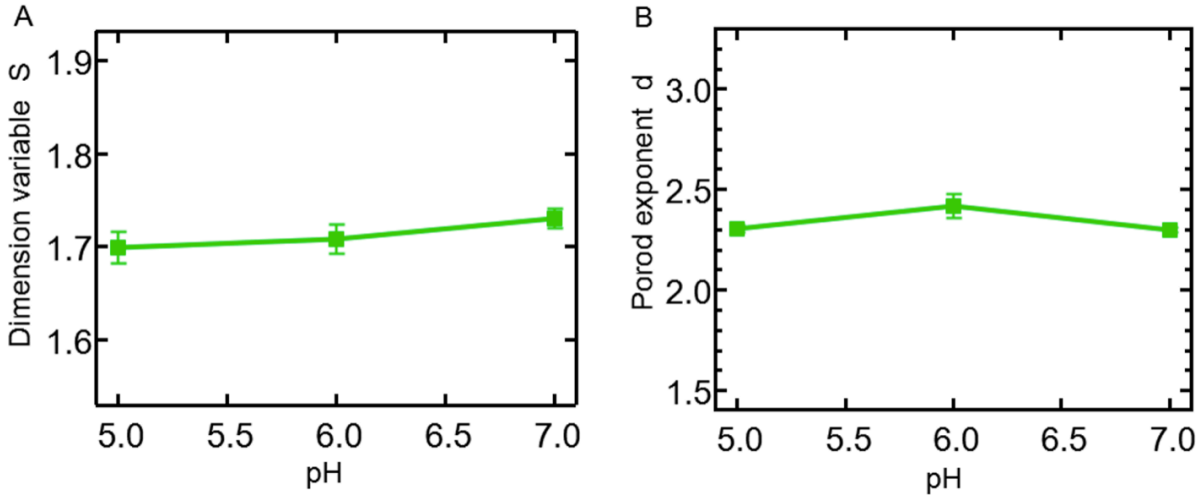

Figure S8: Aggregate shape parameters determined from SAXS data. A: Dimension variable *S,* and B: Porod exponent *d* as a function of pH. The data shows that neither the dimension variable *S* (A) nor the Porod exponent *d* (B) change with pH in the measured range.

The effect of salt and particle concentration on the hydrodynamic diameter of silica nanoparticles determined via DLS

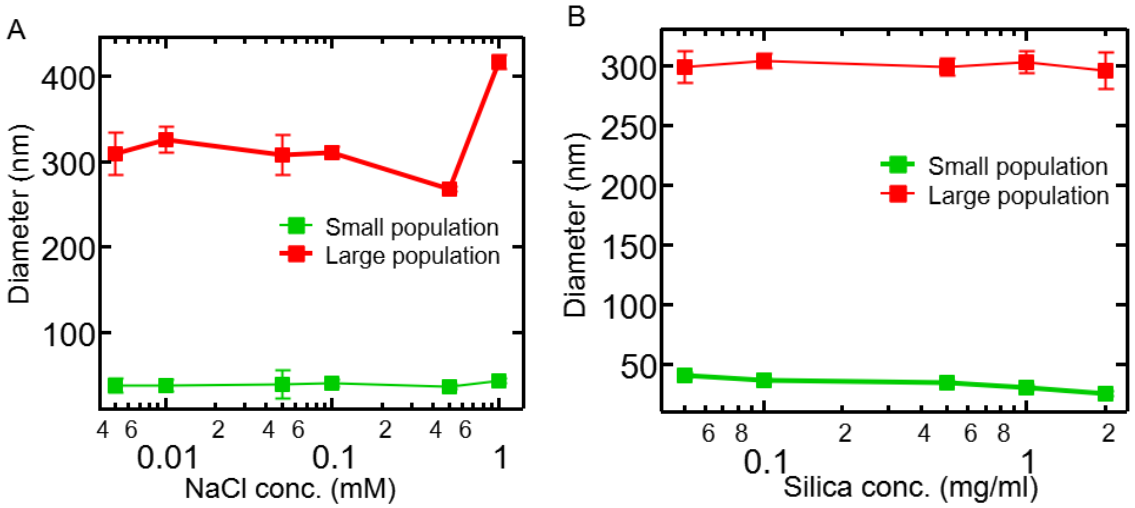

Figure S9: The effect of salt and silica particle concentration concentration on the hydrodynamic diameter determined via DLS. A: The effect of salt concentration on the silica aggregates size (silica concentration is 0.1 mg mL^{-1}). B: The effect of silica concentration on the silica particle diameter determined using DLS at a NaCl concentration of 0.01 mg mL^{-1}.

References

1. A. V. Delgado, F. González-Caballero, R. J. Hunter, L. K. Koopal and J. Lyklema, *Pure and Applied Chemistry*, 2005, **77**, 1753-1805.
2. SasView for Small Angle Scattering Analysis., https://www.sasview.org/).
3. D. K. Carpenter, *Journal of Chemical Education*, 1977, **54**, A430.
4. J. Stetefeld, S. A. McKenna and T. R. Patel, *Biophysical Reviews*, 2016, **8**, 409-427.
5. ALV software for DLS data analysis, https://www.alvgmbh.de).
6. S. W. Provencher and P. Štêpánek, *Particle & Particle Systems Characterization*, 1996, **13**, 291-294.
7. S. W. Provencher, *Computer Physics Communications*, 1982, **27**, 229-242.
8. R. Nixon-Luke and G. Bryant, *Particle & Particle Systems Characterization*, 2019, **36**, 1800388.
9. B. Hammouda, *Journal of Applied Crystallography*, 2010, **43**, 716-719.